Wojciechowski, J. et al.: Enhanced conditioning and disrupted extinction processes in men struggling with compulsive sexual behaviors
https://doi.org/10.1556/2006.2025.00012

SUPPLEMENTARY MATERIALS

Reliability of used questionnaires scales

The reliability of the following questionnaire scales was assessed using Cronbach's α procedure: Brief Pornography Screener (α=0.94), Sexual Addiction Screening Test (α=0.92), Hypersexual Behavior Inventory (α=0.98), Obsessive Compulsive Inventory (α=0.75), Impulsiveness Scale (α=0.77), The Hospital Anxiety and Depression Scale (α=0.81).

Adaptive fMRI task procedure

Each time a trial that was planned to be reinforced (by having a longer window of opportunity period) failed to be reacted upon, a next-in-queue non-reinforced trial was switched to be reinforced in addition to prolonging the window of opportunity length for all following reinforced trials (+20 ms for all reinforced trials and -20ms for all non-reinforced trials, Kruse et al., 2017; Hahn et al., 2009). Likewise, trials that were planned to be non-reinforced and had faster-than-anticipated reaction time resulted in the shortening of future windows and re-queuing trial order so that, in the end, subjects ended up with a near 7:3 ratio of won-to-lost trials. The trial order was semi-randomized so that the same specific condition type and its reinforcement could never be presented twice in a row. Additionally, the first six trials in the first fMRI run were always presented such that in the first three trials, each of the conditions had to appear, and only one trial could be reinforced (either monetary or pornographic); the second three trials also had to have one of each condition and the other condition would be reinforced. The order of those conditions and its reinforcement was randomized between subjects. Thus, the pace of conditioning was normalized between subjects at the beginning of the task. Before entering the MRI and beginning the experiment, subjects underwent a brief training on the task to familiarize themselves with the procedure.

Image acquisition details

Scanning was performed on a 3T Siemens Prisma MRI scanner (Siemens Medical Solutions) using a 64-channel RF head coil. Structural MRI data were acquired with a T1-weighted 3D MP-Rage sequence (TR = 2.4s, TI = 1000ms, TE = 2.74ms, 8° flip angle, matrix 320×320, FOV = 256×256 mm, isometric voxel size 0.8 mm, 240 slices), lasting 6:52 minutes. Functional data was acquired using a Multi-band EPI sequence (TR = 750ms, TE = 31 ms, FA=52°, FOV=220×220 mm, matrix = 110×110, 72 axial slices, isometric 2 mm voxel, no interslice gap, Slice Accel. Factor = 8, In-Plane Accel. Factor = 1, IPAT = 8).

Image preprocessing details

All functional scans had an even number of runs with the opposite phase coding direction (anterior-posterior and posterior-anterior). Spatial distortions were corrected with the FSL *topup* tool based on the average representation of the images in both directions. Functional data was spatially realigned to the mean image, to which the structural image was then co-registered. Segmentation and normalization to the common MNI space were performed based on high-resolution structural images with resampling to 1 mm isometric voxels. The obtained transformation parameters were applied to the functional volumes with resampling to 2 mm isometric voxels. The normalized functional images were spatially smoothed with a Gaussian kernel of full-width half-maximum (FWHM) of 6 mm and 0.004 Hz high-pass filtered.

Statistical modeling of fMRI data

BOLD responses evoked by each cue type ($CS+_{erotic}$, $CS+_{cash}$, CS-) and reward type ($UCS+_{erotic}$, $UCS+_{cash}$, UCS-) were modeled as separate regressors. Additionally, the first occurrence of each trial type was modeled as a single regressor of no interest since it is required to present both the cue and the reward at least once to start the conditioning (and extinction) process (Phelps et al., 2004). The model also included six motion-related nuisance regressors. All four fMRI runs (two conditioning and two extinction) were input into one model on the first level (for each subject). Both conditioning and extinction tasks were divided into early and late phases, naturally occurring in the first and second fMRI run of each task, similar to Kruse et al. (2017) and Banca et al. (2016), with a slight modification of modeling the first seven (out of 10) occurrences of given condition in the early phase and the last seven occurrences in the late phase to increase the potential effects specific to a given conditioning phase. This resulted in four time points: early conditioning, late conditioning, early extinction, and late extinction.

Hardware, software, and stimuli used in the experiment

Explicit erotic stimuli were selected from a subset of the Nencki Affective Picture System (NAPS-ERO) based on the highest arousal and valence scores (Wierzba et al., 2015). The experimental protocol was controlled by the Presentation software (Neurobehavioral Systems Inc.). Stimuli were presented on an MR-compatible full-HD goggle system mounted on a head coil (NordicNeuroLab Inc.). Behavioral responses were collected using MR-compatible response pads (SmitsLab co.).

Whole-brain neuroimaging results

Group differences

Exploratory whole-brain analysis revealed significant differences between CSB and control group only during late conditioning (Fig. S1). The CSB group had lower activity in bilateral calcarine for both $CS+_{erotic}$ vs. CS- and $CS+_{cash}$ vs. CS- in the late conditioning phase, but for $CS+_{erotic}$ vs. CS-, additionally, part of the precuneus, right middle temporal gyrus, right insula, right parahippocampal gyrus and a cluster spanning left hippocampus, fusiform gyrus, and parahippocampal gyrus had lower activity. In $CS+_{erotic}$ vs. CS-, the CSB group additionally had higher activation in a cluster located in the right cerebellum and inferior temporal gyrus. Results are presented in Table S1 and S2.

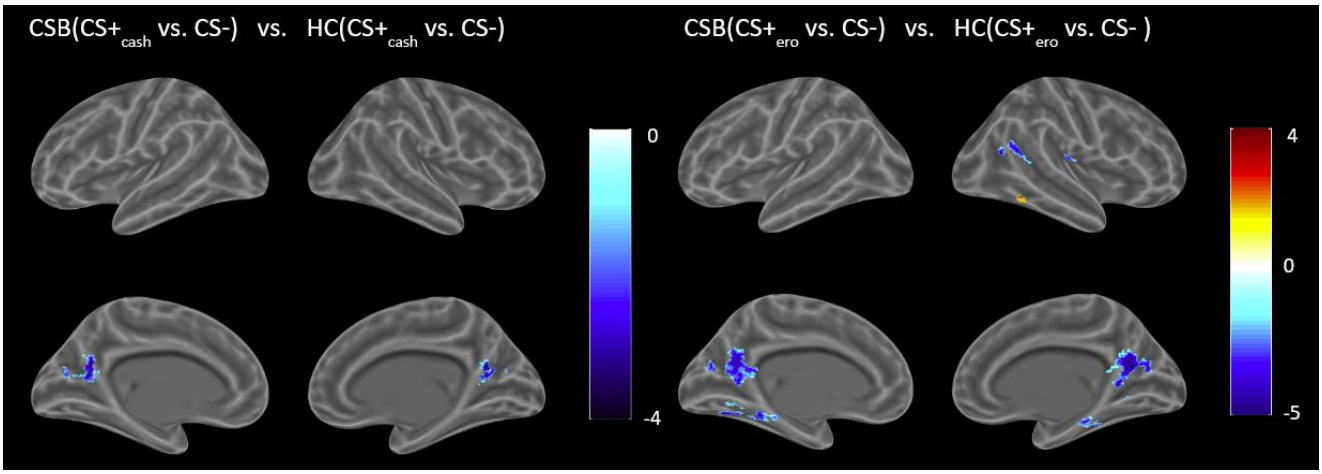

Figure S1. Group differences in BOLD activity in (left) $CS+_{cash}$ vs. CS- and (right) $CS+_{erotic}$ vs. CS- contrasts between the CSB and control groups in late conditioning. The results were obtained using a voxel-level threshold of $p<.001$ and an FWE-corrected cluster-forming threshold of $p< .05$. Color bars represent the *t*-values.

Table S1

Whole-brain results of group differences between CSB and HC in $CS+_{erotic}$ vs. CS- contrast.

					MNI Coordinates		
	Region Name	Side	Cluster size	*t*-value	x	y	z
CSB > HC	Cerebellum 6	R	326	4.97	40	-66	-24
	Inferior Temporal Gyrus	R	326	4.06	60	-54	-16
	Cerebellum (Crus 1)	R	326	3.84	54	-54	-38
HC > CSB	Precuneus	R	1144	5.07	12	-56	18
	Calcarine Gyrus	L	1144	4.22	-16	-56	10
	Middle Temporal Gyrus	R	240	4.87	40	-52	18
	Insula Lobe	R	124	4.84	32	-20	22
	Fusiform Gyrus	L	311	4.82	-28	-38	-10
	ParaHippocampal Gyrus	L	311	4.37	-24	-20	-18
	ParaHippocampal Gyrus	R	135	4.64	30	-28	-14

Cluster extent-based correction (FWEc) p< .05. The AAL3 atlas was used to denote region names. Clusters with peaks more than 8mm apart have indicated several regions per cluster.

Table S2

Whole-brain results of group differences between CSB and HC in $CS+_{cash}$ vs. CS- contrast.

					MNI Coordinates		
	Region Name	Side	Cluster size	*t*-value	x	y	z
HC > CSB	Calcarine Gyrus	R	186	4.77	8	-60	18
	Calcarine Gyrus	L	234	4.75	-4	-64	14

Cluster extent-based correction (FWEc) p< .05. The AAL3 atlas was used to denote region names.

General conditioning effects

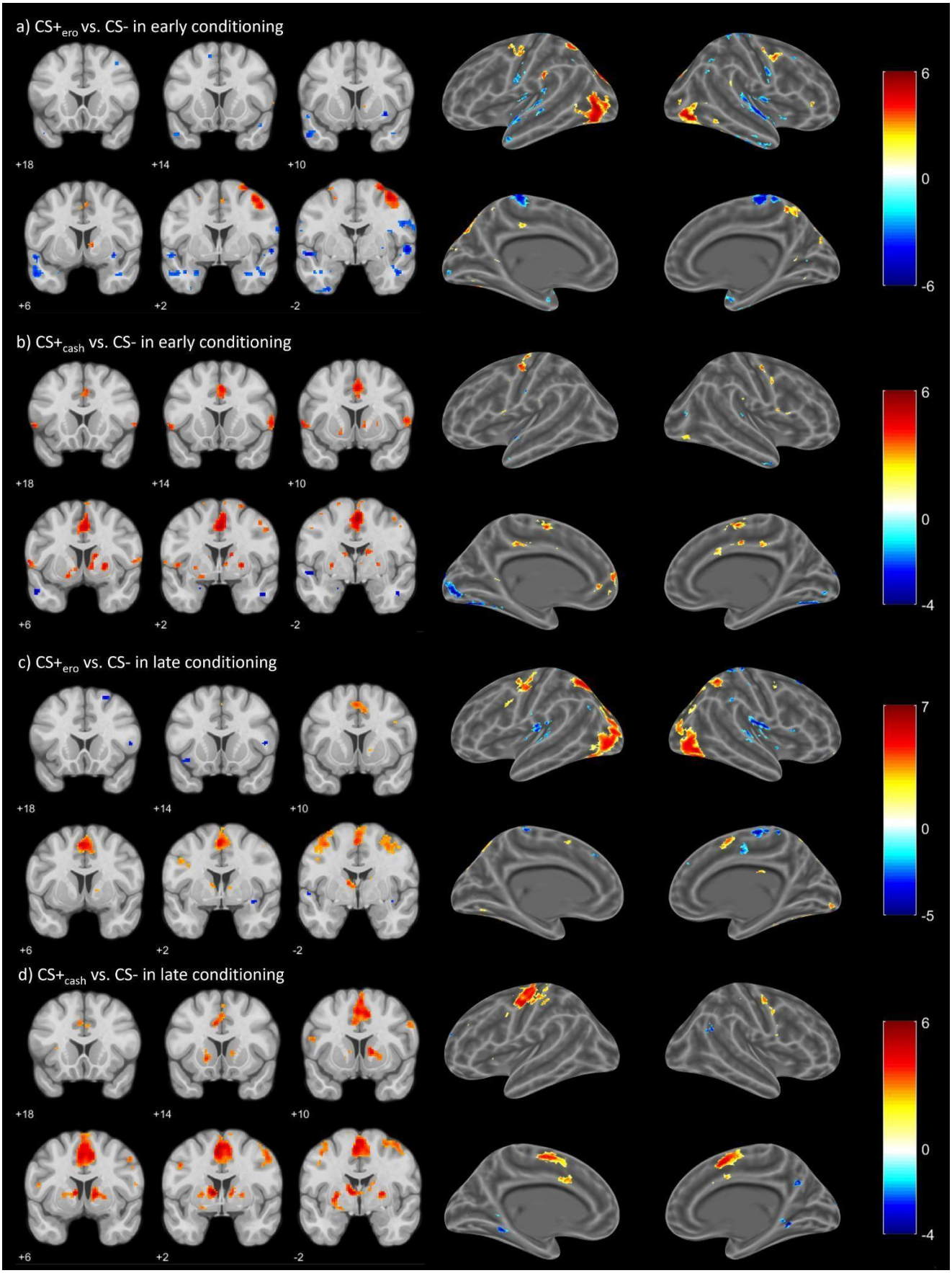

Figure S2. Effects of conditioning on BOLD activity for four analyzed contrasts (a-d), for all participants pooled together. For each contrast, left panels present coronal planes of volumetric representation of subcortical activity (see x coordinates in MNI space below each map); right panels present a surface render of cortical activity. Color bars represent *t*-values for both volumetric and surface visualizations; threshold used is p< .001.

General extinction effects

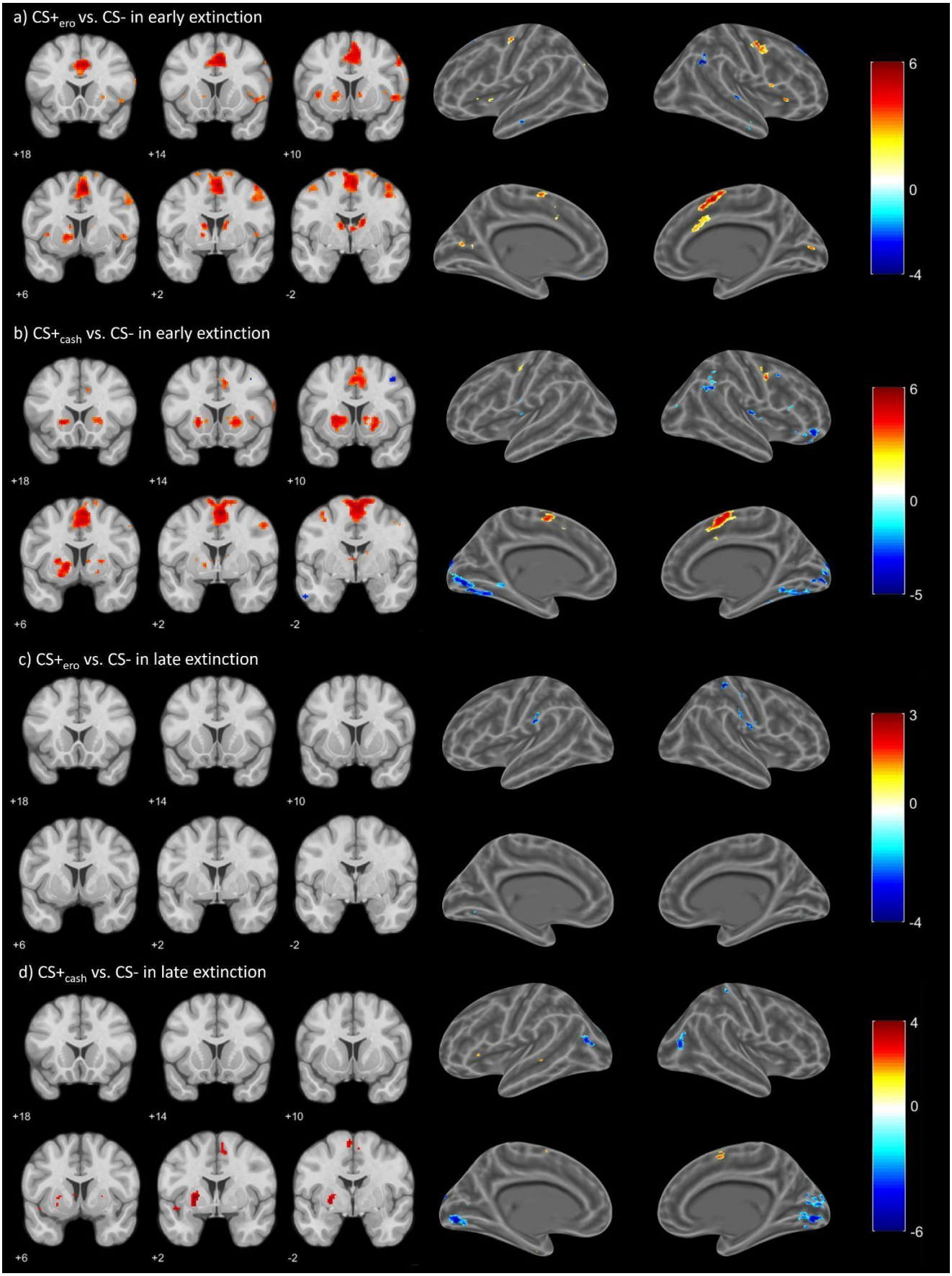

Figure S3. Effects of extinction on BOLD activity for four analyzed contrasts (a-d), for all participants pooled together. For each contrast, left panels present coronal planes of volumetric representation of subcortical activity (see x coordinates in MNI space below each map); right panels present a surface render of cortical activity. Color bars represent *t*-values for both volumetric and surface visualizations; threshold used is p< .001.

LITERATURE

Banca, P., Morris, L. S., Mitchell, S., Harrison, N. A., Potenza, M. N., & Voon, V. (2016). Novelty, conditioning and attentional bias to sexual rewards. *Journal of Psychiatric Research*, *72*, 91–101. https://doi.org/10.1016/j.jpsychires.2015.10.017

Hahn, T., Dresler, T., Ehlis, A.-C., Plichta, M. M., Heinzel, S., Polak, T., Lesch, K.-P., Breuer, F., Jakob, P. M., & Fallgatter, A. J. (2009). Neural response to reward anticipation is modulated by Gray's impulsivity. *NeuroImage*, *46*(4), 1148–1153. https://doi.org/10.1016/j.neuroimage.2009.03.038

Kruse, O., Tapia León, I., Stark, R., & Klucken, T. (2017). Neural correlates of appetitive extinction in humans. *Social Cognitive and Affective Neuroscience*, *12*(1), 106–115. https://doi.org/10.1093/scan/nsw157

Wierzba, M., Riegel, M., Pucz, A., Leśniewska, Z., Dragan, W. Ł., Gola, M., Jednoróg, K., & Marchewka, A. (2015). Erotic subset for the Nencki Affective Picture System (NAPS ERO): Cross-sexual comparison study. *Frontiers in Psychology*, *6*, 145137. https://doi.org/10.3389/fpsyg.2015.01336